How to cite: *Angew. Chem. Int. Ed.* **2020**, *59*, 16241 – 16246
International Edition: doi.org/10.1002/anie.202004812
German Edition: doi.org/10.1002/ange.202004812

Polypnictogen Complexes

Iodination of *cyclo*-E_5-Complexes (E = P, As)

*Helena Brake, Eugenia Peresypkina, Alexander V. Virovets, Martin Piesch, Werner Kremer, Lisa Zimmermann, Christian Klimas, and Manfred Scheer**

Dedicated to Professor Todd Marder on the occasion of his 65th birthday

Abstract: *In a high-yield one-pot synthesis, the reactions of $[Cp^*M(\eta^5\text{-}P_5)]$ (M = Fe (**1**), Ru (**2**)) with I_2 resulted in the selective formation of $[Cp^*MP_6I_6]^+$ salts (**3**, **4**). The products comprise unprecedented all-cis tripodal triphosphino-cyclotriphosphine ligands. The iodination of $[Cp^*Fe(\eta^5\text{-}As_5)]$ (**6**) gave, in addition to $[Fe(CH_3CN)_6]^{2+}$ salts of the rare $[As_6I_8]^{2-}$ (in **7**) and $[As_4I_{14}]^{2-}$ (in **8**) anions, the first di-cationic Fe-As triple decker complex $[(Cp^*Fe)_2(\mu,\eta^{5:5}\text{-}As_5)][As_6I_8]$ (**9**). In contrast, the iodination of $[Cp^*Ru(\eta^5\text{-}As_5)]$ (**10**) did not result in the full cleavage of the M–As bonds. Instead, a number of dinuclear complexes were obtained: $[(Cp^*Ru)_2(\mu,\eta^{5:5}\text{-}As_5)][As_6I_8]_{0.5}$ (**11**) represents the first Ru-As_5 triple decker complex, thus completing the series of monocationic complexes $[(Cp^RM)_2(\mu,\eta^{5:5}\text{-}E_5)]^+$ (M = Fe, Ru; E = P, As). $[(Cp^*Ru)_2As_8I_6]$ (**12**) crystallizes as a racemic mixture of both enantiomers, while $[(Cp^*Ru)_2As_4I_4]$ (**13**) crystallizes as a symmetric and an asymmetric isomer and features a unique tetramer of {AsI} arsinidene units as a middle deck.*

Introduction

As a step in the synthesis of organophosphorus compounds, the chlorination of white phosphorus (P_4) still is an industrially relevant process, in which PCl_3 or PCl_5 are formed and subsequently derivatized to give the desired products that act for example, as additives in fertilizers, detergents and food.[1] Very recently, the detailed mechanism of the complete iodination of P_4 to four equivalents of PI_3 was postulated based on DFT analyses, describing each step as a concerted reaction rather than a redox reaction.[2] Before, Tattershall and Kendall had studied halogenations of white phosphorus thoroughly by performing ^{31}P NMR investigations on the reaction mixtures.[3] In those reactions of P_4 with Br_2 or I_2, besides larger amounts of PX_3 and P_2X_4, also P_4Br_2 and P_7X_3 (X = Br, I (**A**)) are formed (Scheme 1a). In general, while P_4X_2 butterfly compounds were detected only for X = Cl, Br, the P_7X_3 cage compound was rather formed for X = I. However, the products were merely detected spectroscopically, and a synthetic access was not given. Moreover, iodine is not only known to accelerate the transformation of white phosphorus to red phosphorus, but also to contribute to the transformation of red phosphorus to its black allotrope.[4] In both the formation of the P_7I_3 cage and the allotropic transformations of phosphorus, besides the cleavage, also the recombination of the P–P bonds must take place. Hence, the question arises if novel polyphosphorus frameworks can also be synthesized by reactions of polyphosphorus complexes with I_2. Nevertheless, such investigations are rare and limited to P_4 complexes. While the reaction of an η^1-P_4 complex with I_2 gives four equivalents of PI_3, one of which stays coordinated to the metal center,[5] the reaction of $[Ag(\eta^2\text{-}P_4)_2][TEF]$ ($TEF^- = Al\{OC(CF_3)_3\}_4^-$) with I_2 at −78 °C affords the binary phosphorus-rich cation $[P_5I_2]^+$ (**B**), which reacts further above −40 °C to give $P_3I_6^+$ (**C**) as the first subvalent binary P–X cation (Scheme 1b).[6] In 2012, Stop-

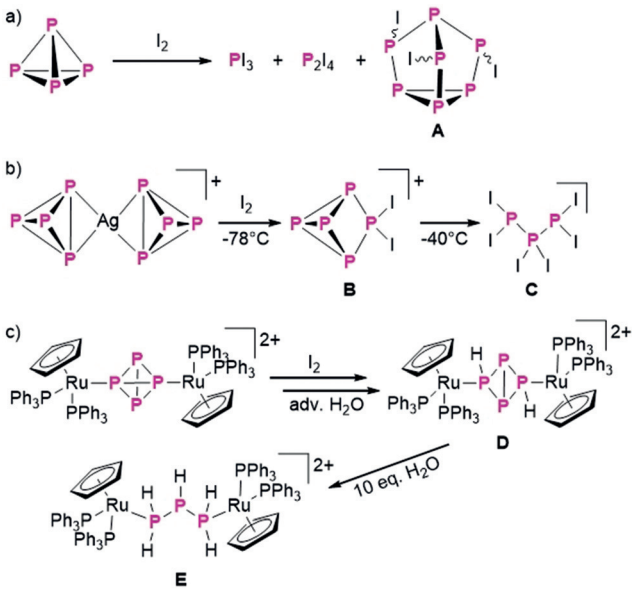

Scheme 1. Selected examples of iodination reactions as a route to novel polyphosphorus frameworks.

[*] H. Brake, Dr. E. V. Peresypkina, Dr. A. V. Virovets, M. Piesch, L. Zimmermann, C. Klimas, Prof. Dr. M. Scheer
Institute of Inorganic Chemistry, University of Regensburg
93040 Regensburg (Germany)
E-mail: manfred.scheer@ur.de
Homepage: https://www.uni-regensburg.de/chemie-pharmazie/anorganische-chemie-scheer/startseite/index.html
Prof. Dr. W. Kremer
Institute of Biophysics and Physical Biochemistry,
University of Regensburg
93040 Regensburg (Germany)
Supporting information and the ORCID identification number(s) for the author(s) of this article can be found under: https://doi.org/10.1002/anie.202004812.

pioni et al. reported on the synthesis of a bridging P_4H_2 butterfly ligand complex **D** from a bridging P_4 complex by reaction with I_2 and adventitious water. Further hydrolysis afforded a bridging P_3H_5 ligand in **E**, releasing phosphorous acid (Scheme 1c). Both the P_4H_2 butterfly and the linear P_3H_5 ligand had until then been unprecedented.[7] These examples clearly show the potential of iodinating P_4 and its complexes for the synthesis of unprecedented polyphosphorus moieties. Thus, the question arises as to what interesting new products may be expected when polypnictogen complexes other than P_4 complexes are iodinated. Surprisingly, such investigations have been left untouched so far.

Herein, we report on the iodination of the *cyclo*-E_5 complexes $[Cp^*M(\eta^5\text{-}E_5)]$ (M = Fe, Ru; E = P,[8] As) to establish iodination reactions as a general method in polypnictogen chemistry to obtain unprecedented E-I-containing cage compounds and ligands.

Results and Discussion

Layering a CH_2Cl_2 solution of $[Cp^*Fe(\eta^5\text{-}P_5)]$ (**1**) with three equivalents of I_2 dissolved in CH_3CN afforded small black needles of $[Cp^*FeP_6I_6]I$ (**3-I**) and $[Cp^*FeP_6I_6](I)_{0.5}(I_3)_{0.5}$ (**3-I_3**) (Scheme 2). Upon drying of **3-I_3** or mixtures thereof, I_2 was evaporated out of the crystals leaving pure **3-I** in 79% yield. Applying an excess of I_2 (9 equiv.) affords PI_3 in addition to crystalline **3-I_3**. Analogously, the layering reaction of $[Cp^*Ru(\eta^5\text{-}P_5)]$[9] (**2**) with three equivalents of I_2 resulted in $[Cp^*RuP_6I_6]I$ (**4**) as metallic black needles in 84% yield (Scheme 2).

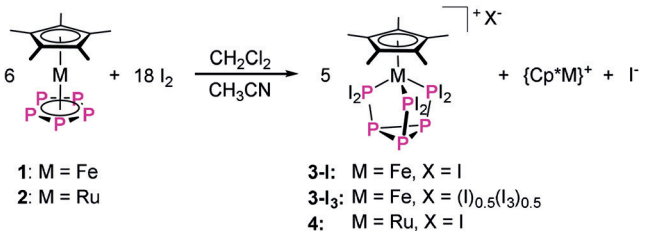

Scheme 2. Reactions of $[Cp^*M(\eta^5\text{-}P_5)]$ (M = Fe (**1**), Ru (**2**)) with I_2.

The fate of the respective {Cp*M} fragments could not be clarified, even though $[FeCp^*_2]^+$ was detected in the ESI-MS spectrum of the mother liquor of the reaction with M = Fe. Furthermore, the interception of the {Cp*M} fragments by another equivalent of $[Cp^*M(\eta^5\text{-}P_5)]$ (**1** or **2**) to form the triple decker cations $[(Cp^*M)_2(\mu,\eta^{5:5}\text{-}P_5)]^+$ is conceivable. In fact, in the $^{31}P\{^1H\}$ NMR spectrum of the mother liquor of the reaction with M = Fe, a signal at −18.6 ppm was detected, comprising a chemical shift similar to that of other known $[(Cp^RFe)_2(\mu,\eta^{5:5}\text{-}P_5)]^+$ salts $([Cp^*Fe)_2(\mu,\eta^{5:5}\text{-}P_5)][BF_4]$:[10] δ_P = −23.0 ppm; $[CpFe(\mu,\eta^{5:5}\text{-}P_5)FeCp^*][PF_6]$:[11] δ_P = −15.8 ppm).

Alternatively, **3-I** can be synthesized more easily by stirring both starting materials pre-dissolved in CH_2Cl_2 and CH_3CN, where the $[Cp^*FeP_6I_6]^+$ salts (**3**) precipitated immediately as an insoluble black microcrystalline powder. After drying, its composition and purity were confirmed by elemental analysis and X-ray powder diffraction, respectively (Figure 1).

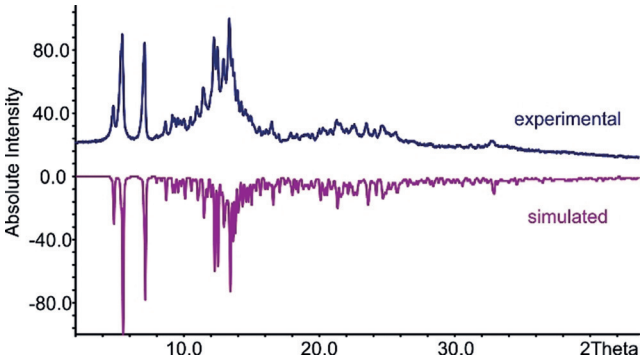

Figure 1. Experimental (top) X-ray powder diffraction pattern of precipitated $[Cp^*FeP_6I_6]I$ (**3-I**) in comparison to the diffraction pattern (bottom) simulated from the single-crystal X-ray data of **3-I**.

The molecular structures of **3-I**, **3-I_3** and **4** (Figure 2) each reveal a tripodal *cyclo*-$P_3(PI_2)_3$ ligand coordinating to the {Cp*M} fragment thus capping the three PI_2-groups, with the resulting MP_6 core resembling the nortricyclane structure of P_7^{3-}.[12] Interestingly, a related *cyclo*-$P_3(P^tBu_2)_3$ ligand was reported by Fritz et al., acting as a bridging ligand towards two Ni centers.[13] However, in contrast to **3** and **4**, the phosphino-substituents in *cyclo*-$P_3(P^tBu_2)_3$ are not arranged all-*cis*, thus impeding the formation of mononuclear complexes. Moreover, Fenske reported on the cluster $[(Cp^*Fe)_3\{(\eta^3\text{-}P_3)Fe\}P_6]$ comprising an all-*cis* arranged *cyclo*-$P_3(P)_3$ core but with capping Cp*Fe units.[14]

Therefore, compounds **3** and **4** represent unprecedented examples of free metallo-nortricyclane derivatives. The P–P bond lengths in **3-I**, **3-I_3** and **4** each are in the range of P–P single bonds (2.22 Å),[15] with the endocyclic bonds (2.160(6) Å–2.234(9) Å) being somewhat shorter than the exocyclic ones (2.245(4) Å–2.281(7) Å). The exocyclic P–P bonds in **3** and **4** are also longer than the P–P bonds between the basal and the equatorial P atoms in C_3 symmetric P_7R_3-nortricyclan structures (2.1709(4)–2.229(1) Å),[16a,b] but comparable to the exocyclic P–P bond lengths in the *cyclo*-$P_3(P^tBu_2)_3$ ligand (2.259(1)–2.276(1) Å).[13d] While the endocyclic P–P bond lengths for **3-I** and **4** (2.199(9)–2.234(9) Å) are comparable to the bond lengths between the basal P atoms of P_7R_3 nortricyclan structures (2.2021(7)–2.244(11) Å)[16c,d] and to the endocyclic P–P bond lengths of the *cyclo*-$P_3(P^tBu_2)_3$ ligand (2.199(1)–2.208(1) Å),[13d] two of the endocyclic P–P bond lengths of **3-I_3** are shorter (2.160(6), 2.187(7) and 2.210(6) Å). Interestingly, in all three structures, close P···I^- contacts between the I^- counterions and P atoms of the P_3 cycles are found with distances of 3.395(3) Å to 3.666(5) Å being smaller than the sum of the van-der-Waals radii (3.78 Å).[17] While for **3-I** and **4** the average distances are especially short, in **3-I_3** it is slightly longer and the I^- counterion interacts with P atoms of two P_3 cycles compared to one as in **3-I** and **4** (Figure 2a–c). Similar P···I^- distances (3.426(1) Å) are also found for a *P*-Iodo-substituted N-heterocyclic phosphine (I-NHP), in which the P···I interaction was described as predominantly ionic.[18] The significantly

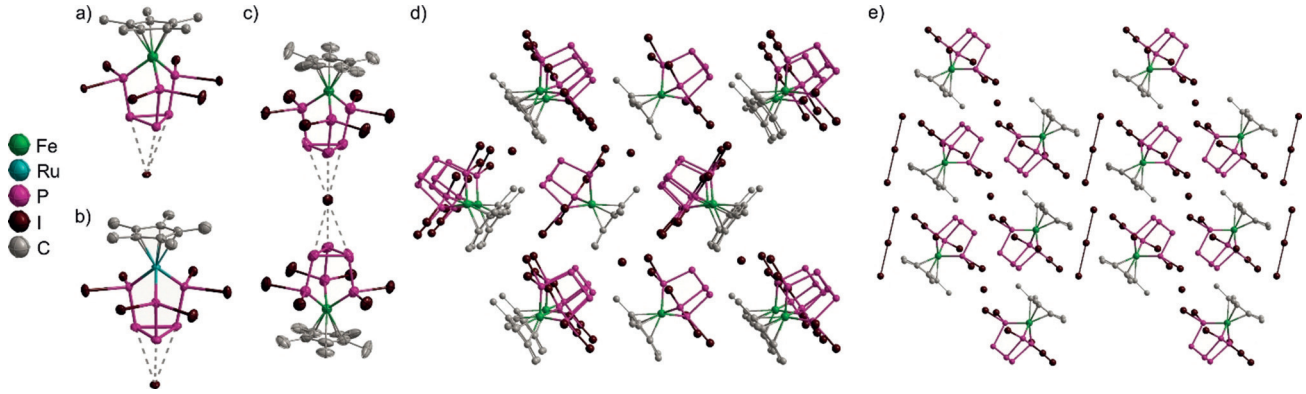

Figure 2. Molecular structures with shortened P···I contacts of a) $[Cp^*FeP_6I_6]I$ (**3-I**); b) $[Cp^*RuP_6I_6]I$ (**4**); c) $[Cp^*FeP_6I_6](I)_{0.5}(I_3)_{0.5}$ (**3-I_3**). A.d.p. ellipsoids at 50% probability level and H atoms omitted for clarity. Crystal packing in d) $[Cp^*FeP_6I_6]I$ (**3-I**) and e) $[Cp^*FeP_6I_6](I)_{0.5}(I_3)_{0.5}$ (**3-I_3**) drawn in the ball-and-sticks model with view along the crystallographic *b* axis.[30]

shortened $I^-\cdots I$ specific contacts between the I^- counterion and two iodine atoms of the PI_2 ligands of two different $[Cp^*FeP_6I_6]^+$ cations (3.3523(9) and 3.535(1) Å (**3-I**); 3.336(2) and 3.508(2) Å (**4**); *cf.* sum of the van-der-Waals radii 3.96 Å)[17] give rise to different 3D networks for **3-I** and **4** in the solid state. In a similar way, the $[Cp^*FeP_6I_6]^+$ cations in **3-I_3** participate in $I^-\cdots I$ specific contacts of 3.545(1) Å with terminal atoms of the I_3^- counter anion (Figures S39–S41, Supporting Information).

Compounds **3** and **4** are insoluble in all common solvents (pentane, toluene, CH_2Cl_2, CH_3CN and thf). Moreover, **3** is insoluble in 1,4-dioxane, dme, CS_2, liquid SO_2, whereas it is soluble under decomposition in dmso, DMF, NMP, HMPA (PI_3 and **1** detected in the $^{31}P\{^1H\}$ NMR spectra). Attempts to obtain a soluble $[Cp^RFeP_6I_6]^+$ salt by a) anion exchange of **3-I** with TlTEF and b) reaction of $[Cp^{BIG}Fe(\eta^5\text{-}P_5)]$[19] ($Cp^{BIG} = C_5(p\text{-}C_6H_4{}^n\text{Bu})_5$) with I_2 only resulted in the formation of PI_3. These facts suggest that the $[Cp^*FeP_6I_6]^+$ cation might be unstable in solution. Therefore, solid state $^{31}P\{^1H\}$ NMR magic angle spinning (MAS) spectroscopy was carried out on **3** and **4** (Figure 3).

For **3**, two signals are detected at chemical shifts of about +75 ppm (PI_2 groups) and −60 ppm (P_3 cycle) next to rotational sidebands (*, ◆). In the Ru analogue **4**, the corresponding signals are slightly shifted to higher field (+58 ppm and −67 ppm). For a sample of **4**, the spinning frequency was exemplarily adjusted from 11400 Hz (Figure 3d) to 25000 Hz (Figure 3e) allowing the clear assignment of signals vs. rotational sidebands. Furthermore, the crystal packing does not seem to influence the $^{31}P\{^1H\}$ MAS NMR spectrum. While for a) crystals of **3-I_3** were isolated and dried to give **3-I**, in b) powder of **3-I** was used and in c) crystals of **3-I_3** were isolated without significant drying. Nevertheless, the resulting spectra do not exhibit any substantial differences.

In the solid state EI-MS spectrum of **3-I** and **4**, only the respective pentaphosphametallocenes $\mathbf{1}^{+\bullet}$ and $\mathbf{2}^{+\bullet}$ as well as $I_2^{+\bullet}$ were detected, besides $HI^{+\bullet}$, $I^{+\bullet}$, $PI_3^{+\bullet}$ and $P_2I_4^{+\bullet}$, thus further confirming the high sensibility of the $[Cp^*MP_6I_6]^+$ cations.

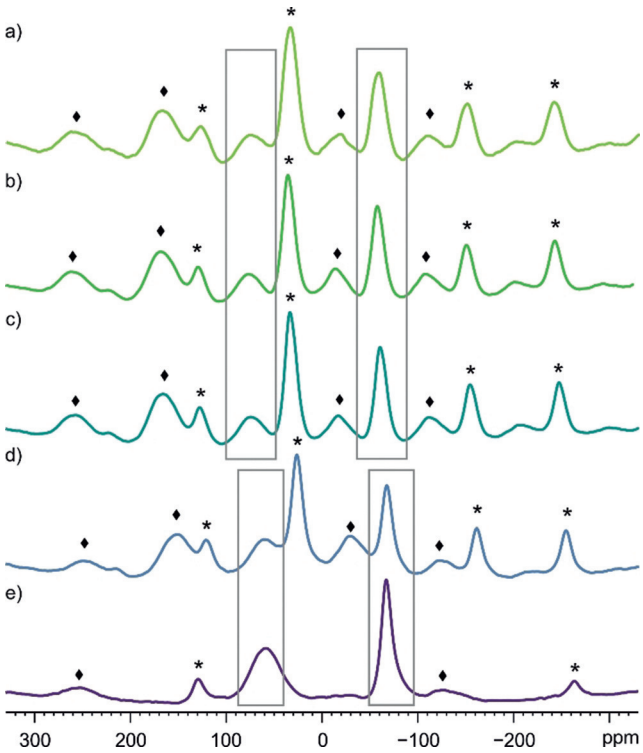

Figure 3. $^{31}P\{^1H\}$ MAS NMR spectra of a) dried crystals of **3-I_3**; b) powder of **3-I**; c) undried crystals of **3-I_3**; d) powder of **4**, each recorded at 11400 Hz MAS frequency and e) $^{31}P\{^1H\}$ MAS NMR spectrum of powder of **4** recorded at 25000 Hz MAS frequency. Rotational sidebands are marked with * or ◆, signals are highlighted by grey boxes.

DFT computations of the frontier molecular orbitals of **3-I** (B3LYP/def2-SVP level of theory, Figure S51, Supporting Information) show that the HOMO as well as the LUMO are mainly located on the P_6I_6 ligand. The HOMO displays formally a linear combination of p orbitals of the iodine substituents, while the LUMO predominantly shows antibonding character between the P and I atoms (formally σ*). Therefore, a nucleophilic attack on the P–I bonds becomes conceivable.

So far, subsequent reactions of **3-I** have mostly led to the re-reduction of the $[Cp^*FeP_6I_6]^+$ cation, as $[Cp^*Fe(\eta^5\text{-}P_5)]$ (**1**) was detected in the $^{31}P\{^1H\}$ NMR spectra of the reactions with KC_8, $[CoCp_2]$, NaCp, LiCp*, $LiAlH_4$, $NaBH_4$, KH, RLi (R = Me, ^{n}Bu, ^{t}Bu), $[Cp''_2Zr(\eta^{1:1}\text{-}P_4)]$. Cyclovoltammetry measurements in the solid state confirmed the possibility of reducing **3-I** (Figure S37, Supporting Information).

Halogen exchange reactions of **3-I** with KF or AgF resulted in disproportionations to give **1** and the PF_6^- anion. Interestingly, **3-I** is soluble in CH_3OH, but a reaction occurs. The ESI-MS spectrum of the resulting solution suggests the formation of $[Cp^*FeP_6(OCH_3)_6]I$ (**5**, Scheme 3), with $[Cp^*FeP_6(OCH_3)_{6-x}H_x]^+$ ($x = 1$–3) fragments being detected as well, which could be side-products or just as well fragmentation products of **5** (cleavage of 1–3 molecules of CH_2O) under mass spectrometric conditions.

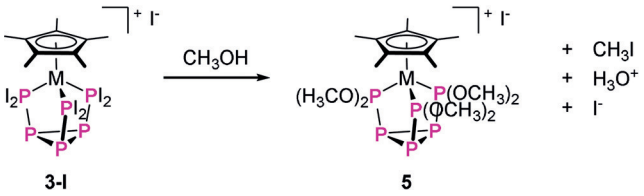

Scheme 3. Reaction of $[Cp^*FeP_6I_6]I$ (**3-I**) with CH_3OH.

The $^{31}P\{^1H\}$ NMR spectrum of the reaction mixture (cf. Scheme 3) shows two multiplets at 285 ppm and −152 ppm (Figure S34, Supporting Information). **5** is formed faster (30 minutes instead of overnight stirring) when **3-I** is reacted with $NaOCH_3$ in CH_3OH, and the subsequent extraction with CH_2Cl_2 leaves a colorless precipitate (presumably NaI). Unfortunately, this reaction is less selective and numerous attempts to crystallize **5** failed.

After exploring the iodination reactions of the P-containing complexes, the question arose as to what would happen when As-containing complexes were used instead. The heavier homologue of pentaphosphaferrocene, $[Cp^*Fe(\eta^5\text{-}As_5)]$[20] (**6**), shows similar redox events in the cyclic voltammogram, with, however, its reactivity towards KH differing significantly.[21] Hence, similarly to the synthesis of **3-I**, the iodination reaction of the arsenic analogue $[Cp^*Fe(\eta^5\text{-}As_5)]$ (**6**) was carried out. The obtained single crystals, as products of a concomitant crystallization, were characterized by X-ray diffraction revealing the structures of $[Fe(CH_3CN)_6][As_6I_8]$ (**7**, Figure S43, Supporting Information), $[Fe(CH_3CN)_6][As_4I_{14}]$ (**8**, Figure S44, Supporting Information) and $[(Cp^*Fe)_2(\mu,\eta^{5:5}\text{-}As_5)][As_6I_8]$ (**9**) (Scheme 4).

While, during the formation of **7** and **8**, a complete cleavage of the Fe−As bonds must have taken place, **9** is notably the first example of a di-cationic Fe-As triple decker complex (Figure 4).

The As−As bond lengths within the 29 VE triple decker di-cation of **9** (2.380(5) Å–2.392(6) Å) range between a normal single (2.42 Å) and a double bond (2.28 Å).[15] When compared to the monocationic triple decker complexes $[CpFe(\mu,\eta^{5:5}\text{-}As_5)FeCp^*][PF_6]$[20] (av. 2.328 Å) and $[Cp^{Bn}Fe)_2(\mu,\eta^{5:5}\text{-}As_5)][BF_4]$[22] (av. 2.34 Å), the As−As bonds

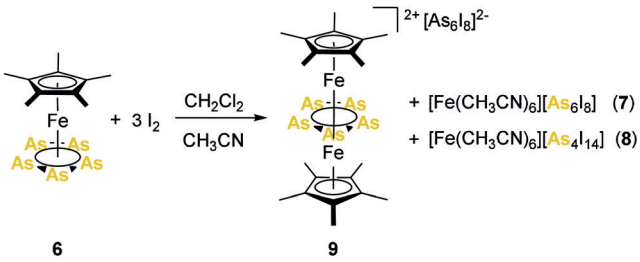

Scheme 4. Reaction of $[Cp^*Fe(\eta^5\text{-}As_5)]$ (**6**) with I_2.

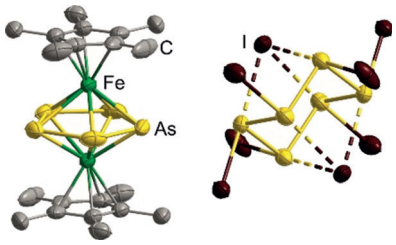

Figure 4. Molecular structure of **9** (incl. counterion). A.d.p. ellipsoids at 50% probability level and H atoms omitted for clarity.[30]

in **9** are slightly elongated. The Fe···Fe distance in **9** (2.795(4) Å) is still longer than the sum of the covalent radii (2.64 Å),[23] but significantly smaller than in the comparable monocations (3.074(3) Å,[20] 3.125(1) Å and 3.1207(9) Å[22]), thus indicating some Fe···Fe bonding interactions. This is further confirmed by a Wiberg bond index (WBI) of 0.38. Moreover, ESR spectroscopy was carried out on crystals of **9**, showing an axial signal with g values of 1.98691 (g(z)) and 1.93421 (g(x,y)), roughly corresponding to one unpaired electron (Figure S38, Supporting Information).

The $[Fe(CH_3CN)_6]^{2+}$ complex cation as well as the $[As_6I_8]^{2-}$ and $[As_4I_{14}]^{2-}$ anions were already structurally characterized as salts with other respective counterions.[24] Therefore, the structures of **7** and **8** will not be discussed hereafter (see Supporting Information for more details). Remarkably, $[As_6I_8]^{2-}$ has so far only been synthesized by the reduction of AsI_3 (either directly or via another As^I iodide reagent),[24b,d] so the reaction according to Scheme 4 represents, for the first time, a formal oxidation of $(As_5)^-$ to this anion. $[As_4I_{14}]^{2-}$ was previously only synthesized by the reaction of grey As and phthalonitrile at 493 K under a stream of I_2 vapor under much harsher conditions.[24c]

In order to prevent the cleavage of the arsenic ligand from the metal center during iodination, I_2 was also allowed to react with $[Cp^*Ru(\eta^5\text{-}As_5)]$[25] (**10**, Scheme 5), with, again, three concomitant crystallization products. Their single crystal X-ray structure analysis revealed the di-nuclear Ru-As complexes $[(Cp^*Ru)_2(\mu,\eta^{5:5}\text{-}As_5)][As_6I_8]_{0.5}$ (**11**), $[(Cp^*Ru)_2As_8I_6]$ (**12**) and $[(Cp^*Ru)_2As_4I_4]$ (**13-sym**) (Figure 5a–c).

Interestingly, $[(Cp^*Ru)_2As_4I_4]$ (**13**) initially crystallized as a symmetric complex (**13-sym**) in the monoclinic $P2_1/n$ space group with all As-I distances being almost equal (2.9453(6) Å–2.9904(6) Å), resulting in a planar $\mu,\eta^{4:4}\text{-}As_4I_4$ middle deck with a four-point star structural motif. This As_4I_4 unit

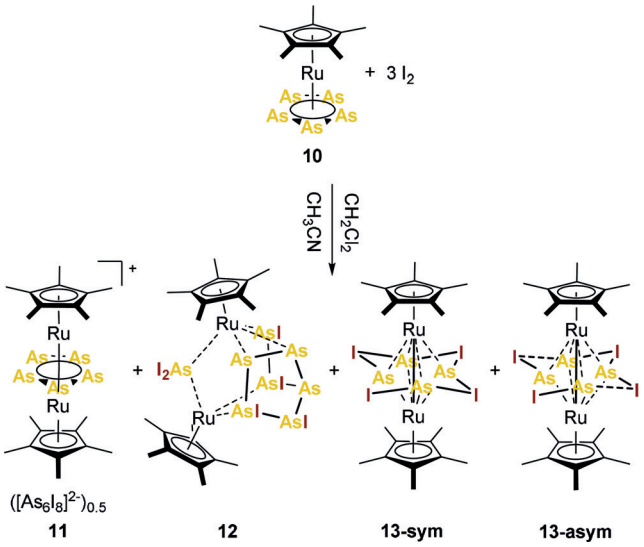

Scheme 5. Reaction of [Cp*Ru(η^5-As_5)] (**10**) with I_2.

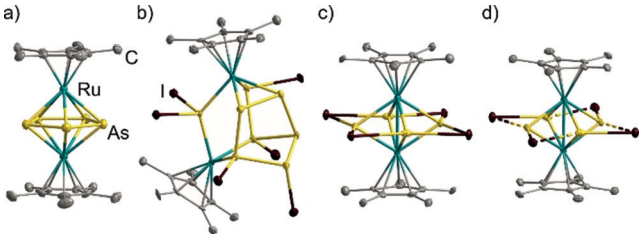

Figure 5. Molecular structures of a) the cation of **11**; b) one enantiomer of **12**; c) **13-sym** and d) **13-asym**. A.d.p. ellipsoids at 50% probability level and H atoms omitted for clarity.[30]

may be interpreted as a tetramer of iodoarsinidene fragments {AsI}. So far, only two examples containing a single bridging {AsI} unit have been reported.[26] After two to four weeks, however, the crystals of all previously mentioned phases stored in the mother liquid had vanished, and instead, another phase of **13** crystallized in the monoclinic *C*2/*c* space group, showing a slightly distorted As_4I_4 ligand in the solid state (**13-asym,** Figure 5d). In **13-asym**, the I atoms are concordantly shifted more to one As to form each a shortened ($d_{As\text{-}I}$ = 2.8591(5) Å–2.8902(5) Å), and an elongated As–I bond ($d_{As\cdots I}$ = 3.0628(5) Å–3.0696(5) Å) as compared to **13-sym**. Nevertheless, all As-I distances are still close to the bond distances in other As-I-As bridges.[27] The Ru-Ru distances in both isomers are similar within experimental error and amount to 2.6594(6) Å (**13-sym**) and 2.6595(7) Å (**13-asym**), being smaller than the sum of the covalent radii (2.92 Å)[23] and close to other reported Ru–Ru bonds.[28] The Ru-As distances (2.4655(6) Å–2.4840(5) Å) are in the range of a single bond (2.46 Å).[15] The As···As distances, ranging from 2.9411(8) Å to 2.9558(8) Å, are smaller than the sum of the van-der-Waals radii (3.70 Å)[17] and the WBIs of 0.21–0.22 (**13-sym**) and 0.20–0.21 (**13-asym**) also suggest weak As···As interactions. Interestingly, no significant I···I intermolecular interactions are found in the solid state and therefore the difference in the structure of the isomers cannot be traced back to this factor (Figure S50, Supporting Information).

DFT computations were carried out in order to determine which structure of **13** is energetically favored, however, the outcome of the geometry optimization is strongly dependent on the used functional and no clear conclusions can be drawn (cf. SI).

Compound **11** crystallizes as red rods in the triclinic space group $P\bar{1}$. Being the first monocationic Ru-As_5 triple decker complex reported, it thus completes the series of monocationic complexes $[(Cp^RM)_2(\mu,\eta^{5:5}\text{-}E_5)]^+$ (M = Fe, Ru; E = P, As). The Ru···Ru distance in **11** (3.3378(9) Å) is larger than the sum of the covalent radii (2.92 Å)[23] and similar to the distance reported for $[(Cp^*Ru)_2(\mu,\eta^{5:5}\text{-}P_5)]^+$ (3.352(1) Å).[29] The As-As distances (2.3649(9) Å–2.3830(8) Å) are in-between a single and a double bond.

Compound **12** crystallizes as a racemic mixture of both enantiomers in the monoclinic space group $P2_1/c$ and is found as a minor phase. It comprises two separate bridging ligands {AsI_2} and {As_7I_4}. All As–I bonds lengths (2.5821(9) Å–2.6703(9) Å) are in accordance with As–I single bonds (2.54 Å).[15] The As–As bonds lengths range between 2.397-(1) Å and 2.481(1) Å and are also in agreement with the expected single bond length (2.42 Å).[15] This is also rather true for the Ru–As bonds (2.375(1) Å–2.542(1) Å; lit.: 2.46 Å).[15]

Conclusion

We showed that the iodination of polypnictogen complexes is a powerful tool for the synthesis of novel types of polypnictogen complexes. The iodination of *cyclo*-As_5 complexes resulted in numerous novel complexes. Of these, the first di-cationic Fe-As triple decker was characterized, revealing further potential in the redox chemistry of polypnictogen complexes. Moreover, for the first time, a monocationic Ru-As_5 triple decker was obtained, thus completing the series of 30VE triple decker complexes $[(Cp^RM)_2(\mu,\eta^{5:5}\text{-}E_5)]^+$ (M = Fe, Ru; E = P, As). Much more remarkable, it was also possible to structurally characterize two different isomers of a complex with a unique tetramer of bridging iodoarsinidene ligands. The iodination of the homologous *cyclo*-P_5 complexes takes place selectively, leading to unprecedented all-*cis* triphosphino-cyclotriphosphine complexes in a high-yield one-pot synthesis. Future investigations will be directed on the halogenation of other polypnictogen complexes, varying the number of heteroatoms in the ligand, the nature of the metal center, the halogen and its source.

Acknowledgements

The Deutsche Forschungsgemeinschaft (DFG) is gratefully acknowledged for the support in the project Sche384/36-1. H.B. is grateful for a PhD fellowship of the Studienstiftung des Deutschen Volkes. Parts of this research (project I-20160654) were carried out at PETRA III at DESY, a member of the Helmholtz Association (HGF). We thank Dr. A.

Burkhardt for the assistance regarding the use of the beamline P11. Open access funding enabled and organized by Projekt DEAL.

Conflict of interest

The authors declare no conflict of interest.

Keywords: arsinidenes · iodination · oxidation · polyphosphorus ligands · polypnictogen complexes

[1] F. Scalambra, M. Peruzzini, A. Romerosa, in *Adv. Organomet. Chem.*, *Vol. 72* (Ed.: P. J. Pérez), Academic Press, San Diego, **2019**, pp. 173 – 222.
[2] C. Mealli, A. Ienco, M. Peruzzini, G. Manca, *Dalton Trans.* **2018**, *47*, 394 – 408.
[3] B. W. Tattershall, N. L. Kendall, *Polyhedron* **1994**, *13*, 1517 – 1521.
[4] a) R. Boulouch, *Compt. Rend.* **1905**, *141*, 256 – 258; b) N. Wiberg, E. Wiberg, A. F. Hollemann, *Anorganische Chemie*, *Vol. 1*, 103rd ed., Walter de Gruyter, Berlin, **2017**, pp. 849 and 853; c) S. Lange, P. Schmidt, T. Nilges, *Inorg. Chem.* **2007**, *46*, 4028 – 4035; d) Z. Zhang, X. Xin, Q. Yan, Q. Li, Y. Yang, T.-L. Ren, *Sci. China Mater.* **2016**, *59*, 122 – 134.
[5] I. De los Rios, J.-R. Hamon, P. Hamon, C. Lapinte, L. Toupet, A. Romerosa, M. Peruzzini, *Angew. Chem. Int. Ed.* **2001**, *40*, 3910 – 3912; *Angew. Chem.* **2001**, *113*, 4028 – 4030.
[6] I. Krossing, *J. Chem. Soc. Dalton Trans.* **2002**, 500 – 512.
[7] P. Barbaro, C. Bazzicalupi, M. Peruzzini, S. Seniori Costantini, P. Stoppioni, *Angew. Chem. Int. Ed.* **2012**, *51*, 8628 – 8631; *Angew. Chem.* **2012**, *124*, 8756 – 8759.
[8] O. J. Scherer, T. Brück, *Angew. Chem. Int. Ed. Engl.* **1987**, *26*, 59; *Angew. Chem.* **1987**, *99*, 59.
[9] O. J. Scherer, T. Brück, G. Wolmershäuser, *Chem. Ber.* **1988**, *121*, 935 – 938.
[10] A. R. Kudinov, D. A. Loginov, P. V. Petrovskii, M. I. Rybinskaya, *Russ. Chem. Bull.* **1998**, *47*, 1583 – 1584.
[11] O. J. Scherer, T. Brück, G. Wolmershäuser, *Chem. Ber.* **1989**, *122*, 2049 – 2054.
[12] W. Dahlmann, H. G. Von Schnering, *Naturwissenschaften* **1972**, *59*, 420.
[13] a) G. Fritz, T. Vaahs, *Z. Anorg. Allg. Chem.* **1987**, *553*, 85 – 89; b) G. Fritz, T. Vaahs, H. Fleischer, E. Matern, *Z. Anorg. Allg. Chem.* **1989**, *570*, 54 – 66; c) G. Fritz, T. Vaahs, H. Fleischer, E. Matern, *Angew. Chem.* **1989**, *101*, 324 – 325; d) H. Krautscheid, E. Matern, J. Olkowska-Oetzel, J. Pikies, G. Fritz, *Z. Anorg. Allg. Chem.* **2001**, *627*, 999 – 1002.
[14] R. Ahlrichs, D. Fenske, K. Fromm, H. Krautscheid, U. Krautscheid, O. Treutler, *Chem. Eur. J.* **1996**, *2*, 238 – 244.
[15] P. Pyykkö, M. Atsumi, *Chem. Eur. J.* **2009**, *15*, 12770 – 12779.
[16] a) D. Weber, C. Mujica, H. G. von Schnering, *Angew. Chem. Int. Ed. Engl.* **1982**, *21*, 863; *Angew. Chem.* **1982**, *94*, 868; b) G. Fritz, E. Layher, H. Goesmann, D. Hanke, C. Persau, *Z. Anorg. Allg. Chem.* **1991**, *594*, 36 – 46; c) K. Schwedtmann, J. Haberstroh, S. Roediger, A. Bauzá, A. Frontera, F. Hennersdorf, J. J. Weigand, *Chem. Sci.* **2019**, *10*, 6868 – 6875; d) G. Fritz, K. D. Hoppe, W. Hönle, D. Weber, C. Mujica, V. Manriquez, H. G. v. Schnering, *J. Organomet. Chem.* **1983**, *249*, 63 – 80.
[17] A. Bondi, *J. Phys. Chem.* **1964**, *68*, 441 – 451.
[18] S. Burck, D. Gudat, M. Nieger, Z. Benkö, L. Nyulászi, D. Szieberth, *Z. Anorg. Allg. Chem.* **2009**, *635*, 245 – 252.
[19] S. Heinl, G. Balázs, M. Scheer, *Phosphorus Sulfur Silicon Relat. Elem.* **2014**, *189*, 924 – 932.
[20] O. J. Scherer, C. Blath, G. Wolmershäuser, *J. Organomet. Chem.* **1990**, *387*, C21 – C24.
[21] M. Schmidt, D. Konieczny, E. V. Peresypkina, A. V. Virovets, G. Balázs, M. Bodensteiner, F. Riedlberger, H. Krauss, M. Scheer, *Angew. Chem. Int. Ed.* **2017**, *56*, 7307 – 7311; *Angew. Chem.* **2017**, *129*, 7413 – 7417.
[22] M. Schmidt, A. E. Seitz, M. Eckhardt, G. Balázs, E. V. Peresypkina, A. V. Virovets, F. Riedlberger, M. Bodensteiner, E. M. Zolnhofer, K. Meyer, M. Scheer, *J. Am. Chem. Soc.* **2017**, *139*, 13981 – 13984.
[23] B. Cordero, V. Gomez, A. E. Platero-Prats, M. Reves, J. Echeverria, E. Cremades, F. Barragan, S. Alvarez, *Dalton Trans.* **2008**, 2832 – 2838.
[24] a) B. A. Stork-Blaisse, G. C. Verschoor, C. Romers, *Acta Crystallogr. Sect. B* **1972**, *28*, 2445 – 2453; b) C. A. Ghilardi, S. Midollini, S. Moneti, A. Orlandini, *J. Chem. Soc. Chem. Commun.* **1988**, 1241 – 1242; c) J. Janczak, R. Kubiak, *Acta Crystallogr. Sect. C* **2003**, *59*, m70 – m72; d) B. D. Ellis, C. L. B. Macdonald, *Inorg. Chem.* **2004**, *43*, 5981 – 5986.
[25] O. J. Scherer, C. Blath, G. Heckmann, G. Wolmershäuser, *J. Organomet. Chem.* **1991**, *409*, C15 – C18.
[26] a) A. Strube, G. Huttner, L. Zsolnai, W. Imhof, *J. Organomet. Chem.* **1990**, *399*, 281 – 290; b) I. Y. Ilyin, S. N. Konchenko, N. A. Pushkarevsky, *J. Cluster Sci.* **2015**, *26*, 257 – 268.
[27] A survey in the Cambridge Crystal Structure Database (CCSD), version 5.40 update 3, 08/2019, revealed 19 As-I-As bridging compounds with a mean As-I distance of 3.043 Å (median 3.077 Å).
[28] a) H. Brunner, B. Nuber, L. Poll, G. Roidl, J. Wachter, *Chem. Eur. J.* **1997**, *3*, 57 – 61; b) D. Carmichael, F. Mathey, L. Ricard, N. Seeboth, *Chem. Commun.* **2002**, 2976 – 2977; c) X. Zhang, Q. Guo, Y. Zhang, Y. Zhang, W. Zheng, *Dalton Trans.* **2018**, *47*, 13332 – 13336.
[29] A. R. Kudinov, D. A. Loginov, Z. A. Starikova, P. V. Petrovskii, M. Corsini, P. Zanello, *Eur. J. Inorg. Chem.* **2002**, 3018 – 3027.
[30] Depositions Numbers CCDC-1985266 (for **3-I**), CCDC-1985259 (for **3-I_3**), CCDC-1985265 (for **4**), CCDC-1985257 (for **7**), CCDC-1985262 (for **8**), CCDC-1985261 (for **9**), CCDC-1985263 (for **11**), CCDC-1985260 (for **12**), CCDC-1985258 (for **13-sym**) and CCDC-1985264 (for **13-asym**) contain(s) the supplementary crystallographic data for this paper. These data are provided free of charge by the joint Cambridge Crystallographic Data Centre and Fachinformationszentrum Karlsruhe Access Structures service www.ccdc.cam.ac.uk/structures.

Manuscript received: April 2, 2020
Revised manuscript received: May 26, 2020
Accepted manuscript online: May 28, 2020
Version of record online: July 9, 2020

